No. 107 (81-8)

Possible Application of the James-Stein Estimator to Several Regression Lines

by

Jack Carpenter[*1]
Motoharu Kimura[*2]
Nozomu Matsubara[*3]

March 1981

*1, *2 Argonne National Laboratery, U. S. A..
*3 The Institute of Socio-Economic Planning, Univ. of Tsukuba.

Abstract

The principle of James-Stein estimator was explained using the most simple case as an example. It is believed that the principle will work for improving the estimation of several regression lines considered as distributed in multivariate normal distribution.

The estimation technique is tried for the regression analysis for Monte Carlo computation data of neutron slowing down spectra. The result showed that if the fit of regression lines was good enough, then not very much room was left for the improvement of fit by James-Stein estimation. If, on the other hand, the data fluctuation was substantially great, the technique certainly brought about the enough improvement in fit.

This result may encourage us to apply to James-Stein technique for improving the regression technique in various fields, when several populations are concerned.

Content

§1. Introduction

The notion of James-Stein Estimator was first introduced on 1960 by C. Stein (1), (2), (3) who pointed out the possibility of improving the usual estimator, sample mean, in the case of multivariate normal (Gaussian) mean. Here an extremely simple example will be presented to explain the basic philosophy of the theory in our framework of the problem. Suppose we have test k test pieces, designated as $j = 1, 2, \ldots k$, of various metals whose length were measured by a certain person using a certain measuring instrument. The length depends on the temperature x. The results of the measurements are shown schematically by the points A_{ij} (.) in Fig. 1. It is not possible to know the true length, f_{ij}, of j th test piece for the value x_i of x and we usually take the estimate y_{ij} by the least square fitting against x (shown by straight line) based on the data points A_{ij} ($i = 1, \ldots n$; $j = 1, \ldots k$), as long as the temperature range is not very large and we can safely assume linear expansion or shrinkage.

coefficient. The measurement for metal A, for example, is independent of the measurements for metal B, C etc and it is quite natural to take separately the least square fitting procedure to each data. We have, however, missed to use some other information obtainable from the data for other test pieces B, C ... . As long as the measurements were executed by the same person and by the same device, the fluctuation of measured results must be ultimately of the same magnitude. The data points for metal A, for example, look rather accurate in some temperature range, but it is plausible that it is just by chance if we look through all the other data points. By taking into account all the data for all other samples simultaneously, we might be able to shift somewhat the data points like the following;

A_{ij} = (The original measurements)

$A_{ij}^{(1)}$ = (A_{ij} shifted vertically in someway)

y_{ij} = ("The regressed value" by the least square fitting to A_{ij} data)

$y_{ij}^{(1)}$ = ("The regressed value" by the least square fitting to $A_{ij}^{(1)}$ data)

We conjecture that when the proper shifting is applied, then the total "risk" might be less. The risks here are defined as follows. If we know the lines ("true" regression lines) ℓ_A, ℓ_B, ℓ_C, ... , which gives the true length f_{ij} of each test piece $j = A, B, C, \ldots$ for the value of $x = x_i$ (or the results of measurement using an instrument

of much better accuracy), we can calculate

$$\text{RISK } 0 = \sum_{j=1}^{k} \sum_{i=1}^{n} (A_{ij} - f_{ij})^2 \tag{1}$$

$$\text{RISK } 1 = \sum_{j=1}^{k} \sum_{i=1}^{n} (A_{ij}^{(1)} - f_{ij})^2 \tag{2}$$

$$\text{RISK } 2 = \sum_{j=1}^{k} \sum_{i=1}^{n} (y_{ij} - f_{ij})^2 \tag{3}$$

$$\text{RISK } 3 = \sum_{j=1}^{k} \sum_{i=1}^{n} (y_{ij}^{(1)} - f_{ij})^2 \tag{4}$$

and if we observe the tendency

$$\text{RISK } 1 \leqq \text{RISK } 0$$

$$\text{RISK } 3 \leqq \text{RISK } 2 \tag{5}$$

then it may be allowed to say that the shifted data points $A_{ij}^{(1)}$ and their regressed values $y_{ij}^{(1)}$ are closer to the true values.

There may exists variety of formulae to find $A_{ij}^{(1)}$ and $y_{ij}^{(1)}$ from the data points A_{ij}, depending on the ways of approximation or simplification in the process of reduction, but the most essential point in this James-Stein proceedure is the introduction of "shrinkage factor ρ," which plays the central role to take into account the fluctuation of measurement in total for the reduction of data of respective element.

The statistical model adopted in this paper is the usual set up of the linear regression analysis. We asssume

$$A_{ij} = f_j(x_i) + \varepsilon_{ij} \qquad (i=1, 2, \ldots, n;\ j=1, \ldots, k) \tag{6}$$

where

$$f_j(x) = \alpha_j + \beta_j(x - \bar{x}), \quad \bar{x} = \Sigma x_i/n$$

and ε_{ij} are random error terms.

It is also assumed that $k > 3$, otherwise the James-Stein procedure is not possible.

The line defined by

$$\ell_j : y = f_j(x) = \alpha_j + \beta_j(x - \bar{x})$$

is the j-th "true regression line." α_j and β_j are estimated by least square estimates

$$a_j = \sum_{i=1}^{n} A_{ij}/n = \bar{A}_j, \quad b_j = \frac{\sum_i (x_i - \bar{x})(A_{ij} - \bar{A}_j)}{\sum_i (x_i - \bar{x})^2}, \tag{7}$$

respectively and the j-th "sample regression line" is given by

$$\hat{\ell}_j : y = a_j + b_j(x - \bar{x})$$

The true value

$$f_{ij} \equiv f_j(x_i) = \alpha_j + \beta_j(x_i - \bar{x}) \tag{8}$$

is then estimated by "regressed value" on the j-th sample regression line

$$y_{ij} = a_j + b_j(x_i - \bar{x}) \tag{9}$$

Under the normality condition of the distribution of ε_{ij};

$$\varepsilon_{ij} \overset{ind}{\sim} \mathcal{N}(0, \sigma^2), \tag{10}$$

b_j and $y_{ij} = a_j + b_j(x_i - \bar{x})$ will also have normal distributions:

$$b_j \sim \mathcal{N}(\beta_j, \sigma^2/\Sigma_i(x_i - \bar{x})^2) \tag{11}$$

$$a_j + b_j(x_i - \bar{x}) \sim \mathcal{N}(\alpha_j + \beta_j(x_i - \bar{x}), \ \sigma^2\left(\frac{1}{n} + \frac{(x_i - \bar{x})^2}{\Sigma_i (x_i - \bar{x})^2}\right)),$$

"sectioned" data at each $x = x_i$, that is, A_{ij} $(j=1, 2, \ldots, k)$ will be processed by the James-Stein procedure (called JSE) to give rise to

$$A_{ij}^{(1)} = \bar{\mu}_i + \rho_i(A_{ij} - \bar{\mu}_i) \tag{12}$$

where

$$\bar{\mu}_i = (\text{average of } y_{ij} \text{ over } j) = \frac{1}{k}\sum_{j=1}^{k} y_{ij} \tag{13}$$

and ρ_i is the shrinkage factor given by

$$\rho_i = 1 - \frac{(k-3)}{(k-1)} \frac{\sigma^2\{\frac{1}{n} + (x_i - \bar{x})^2/\Sigma_i(x_i - \bar{x})^2\}}{\Sigma_j(y_{ij} - \frac{1}{k}\Sigma_j y_{ij})^2} \tag{14}$$

ρ_i are usually less than 1 and have a function to smear out the fluctuation possibly contained in the data set A_{ij}. It is understandable that the larger A_{ij} have larger chance to have fluctuated to the possitive side from the true value and the smaller A_{ij} have

larger chance to have fluctuated to the negative side. In case $\rho_i < 0$, we should put it equal to 0.

σ^2 in (14) is replaced by its estimate s^2, the average over j of residual variances s_j^2 from the sample regression lines;

$$s^2 = \frac{1}{k} \sum_{j=1}^{k} s_j^2, \tag{15}$$

$$s_j^2 = \frac{1}{(n-2)} \{ \sum_i (A_{ij} - \bar{y}_j)^2 - \frac{[\sum_i (x_i - \bar{x})(A_{ij} - \bar{y}_j)]^2}{\sum_i (x_i - x)^2} \} \tag{16}$$

We calculate k regression lines and regressed values $y_{ij}^{(1)}$ by the usual least square fitting to JSE processed A_{ij}, $A_{ij}^{(1)}$ ($j=1, 2, \ldots, k$), and define the Figures of Merits (FOM) of James-Stein processing through (1) to (4) as follows;

$$\text{FOM 1} = {}^{\text{RISK 0}}/_{\text{RISK 1}}, \tag{17}$$

$$\text{FOM 2} = {}^{\text{RISK 2}}/_{\text{RISK 3}} \tag{18}$$

FOM 1 and FOM 2 may be of some measure how much the data were improved by such a proceedure.

Some calculations using computer simulation as described below show that both FOM 1 and FOM 2 are larger than 1 and tend to 1 when the measurement of A_{ij} is very accurate. FOM 1 and FOM 2 become quite large in some cases which means several hundred percent improvement on the confidence interval of the result is possible.

§2. Some descriptions of computer experiments

The raw data of neutron spectra for the target-reflector-moderator system of various configurations for IPNS[4], [5] is reproduced in Fig. 2. Here, E is the neutron energy in eV and the abscissa is in log E scale, and I is in the neutron current in some unit and the ordinate is given in log (EI). A_1, A_2, B, C, correspond to different neutron moderator configulation. We will limit our interest to the neutron energy region of 10 eV to 10 KeV where straight lines for Log (EI) vs log E curve look good for the actual shape of the spectra. Even though it was later suggested that there may exist a knick in the curve A and B, it will not be considered now.[5]

In the abscissa, x_i represents the log E_i and was taken as shown in the figure, taking $n = 10$ equally distant points on x axis and fixed.

Hand calculations were made using the formulate (14) - (18), and also using some other formulae which are not given here. The case using (14) for the shrinkage factor gave a reasonable result. However, the values of ρ_i are all very close to 1.0 and not much difference is found by applying James-Stein procedure. This is very reasonable because the fluctuation of all the data points are rather small and there remains not much room that the regression lines are allowed to move. The Monte-Carlo results shown in Fig. 2 (which we call Shasi's results) are already too accurate to allow the JSE procedure workable. The Table I shows a part of the result of hand calculation for James-Stein processing for the region of $x_i = 1, 2 \ldots, 10$

in Fig. 2.

Some computer programs were compiled to make the calculation somewhat more general in form and to understand the problem systematically. In the program, the final results to be obtained after infinite number of trial of Monte-Carlo (or measured by an infinitely accurate instrument) were assumed, which is shown by $k = 12$ straight lines A, B, ..., L ($j=1, 2, \ldots, 12$) in Fig. 3. First 4 lines, A, B, C, D ($j=1, 2, 3, 4$) correspond to regression lines of Shasi's data points for A_1, C, A_2, and B of Fig. 2. (The ordinate was multiplied by 10^3 and given in linear scale.) Other 8 lines E through L ($j=5, 6, \ldots, 12$) were created arbitrarily to make the problem in a more general form. Each of these points on the straight lines are designated by f_{ij}, or AF(I, J) in computer notation, where

$$i = 1, 2, \ldots, 10 \quad \text{and} \quad j = 1, 2, \ldots, 12.$$

We call this set "NOAF 7000" series.

Another artificial data set, named "NOAF 4190" series, was created to confirm an adequate working of the program, that is, tweleve identical horizontal lines:

$$f_{ij} = 0.500000 \qquad (i=1, 2, \ldots, 10; \quad j=1, 2, \ldots, 12)$$

and the difference between the results in two cases were investigated.

Computer printouts give the following results;

(i) Experimental values A_{ij}, or AA(I, J)

(ii) Their regression lines for $j=1, 2, \ldots, 12$

(iii) James-Stein processed values of $A_{ij}^{(1)}$, or AA1(I, J) and their

regression lines

(iv) Graphic plots of A_{ij} and $A_{ij}^{(1)}$

(v) RISK 0, RISK 1, RISK 2, RISK 3, and FOM 1, FOM 2

were tabulated out.

The most important parameter for the present simulation experiments is the effect of the accuracy of measurements for the above quantities. We considered three different cases to simulate the accuracy and put it into the program.

[Uniform case]

We assume, as in the example shown if Fig. 1, all f_{ij} are normalized so that the points will be in [0, 1]. And assume that the measured data A_{ij} are also all confined in [0, 1] even in a very crude measurements. The most simple program to create measured values of various degree of accuracy is to compare f_{ij} with uniform random numbers U_s on [0, 1] (s=0, 2, ..., NHS) for NHS times of repetition, where NHS, Number of History, is some integer ranging from 1 to ∞ (in practice, $\sim$ 1000). NHS are taken as

$$NHS = 2^{(NR - 1)}, \quad NR = 1, 2, 3, \ldots 9. \tag{19}$$

in accordance with the uniform random number generator.

Define

$$Z_s = \begin{cases} 1 & \text{if} \quad f_{ij} \geq U_s \\ 0 & \text{if} \quad f_{ij} < U_s \end{cases},$$

$$A_{ij} = \sum_{s=1}^{NHS} Z_s / NHS.$$

Then

$$Z_s \sim \mathrm{Bi}\ (1,\ f_{ij})$$

and

$$E(A_{ij}) = f_{ij},$$

$$\sigma^2(A_{ij}) = \frac{f_{ij}(1-f_{ij})}{NHS} = 2^{(1-NR)/2} \cdot f_{ij}(1-f_{ij}) \equiv \sigma_U^2 \qquad (20)$$

A_{ij} will be asymptotically distributed in $\mathcal{N}(f_{ij},\ \sigma_U^2)$ as $NHS \to \infty$, but the distribution, for example, when $NHS = 1$, is such that the A_{ij} takes 0 or 1 with the probability of 1 equal to f_{ij}, which is the crudest measurement.

[Normal case]

It may be more reasonable to consider that A_{ij} will be distributed in $N(f_{ij},\ \sigma_G^2)$ for each $(i,\ j)$. The program to simulate such a case is made by simply calling subroutine of the normal random number of specified standard deviation σ_G which specifies the accuracy of measurement.

[Poisson case]

If we consider some other cases than those shown in Fig. 1, it may be better to assume that A_{ij}'s are distributed in Poisson distribution $\mathrm{Po}(\lambda_{ij})$ with the mean λ_{ij}. Indeed, neutron countings may fluctuate under this law and the relative accuracy of the countings is $\sqrt{\lambda_{ij}} / \lambda_{ij} = 1/\sqrt{\lambda_{ij}}$. Computer simulation for such a case is made by calling subroutine of the Poisson random number generator. To postulate,

however, the various crudeness of measurements, we introduce the two-parameter family with the degree of accuracy being adequately independent of the mean. This will be done by taking

$$A_{ij} = Z/\lambda, \quad Z \sim Po(\lambda f_{ij})$$

Then

$$E(A_{ij}) = f_{ij}, \ \sigma^2(A_{ij}) = f_{ij}/\lambda \equiv \sigma_P^2$$

Monte-Carlo results of neutron ditribution may most adequately be simulated by this program.

The computer prints out graphic representations of FOM 1 - 1 and FOM 2 - 1 vs log $\sigma(\sigma = \sigma_U, \sigma_G, \sigma_P)$. Corresponding to the above three cases of random number generator, we have formulated*);

(1) Uniform

$$\sigma_U = 2^{(n - NR)/2} \cdot \sqrt{f_{ij}(1 - f_{ij})} \tag{21}$$

$$NR = 1, 2, \ldots, 9$$

(2) Normal

$$\sigma_G = 2^{(n - NR)} \quad \text{(absolute case)}, \tag{22}$$

and

$$\sigma_G = 2^{(n - NR)} f_{ij} \quad \text{(coefficient-of-variation case)} \tag{22'}$$

(Both cases were computed, but the same results were obtained essentially.)

---

*) n is for shifting the range of survey in the accuracy. Do not be confused with n for the maximum of i. n is usually taken to be 1. Sometimes it was put equal to some other integer to study different range of σ.

(3) Poisson

$$\sigma_P = \sqrt{\frac{f_{ij}}{\lambda}} = 2^{(n - NR)/2} \cdot \sqrt{f_{ij}} \tag{23}$$

where

$$\lambda = 2^{(NR - n)}, \quad NR = 1, \ldots, 7$$

The computer also prints out the RISK 0 (eq.1) and we can calculate the experimental standard deviation from

$$\sigma_{EX} = \sqrt{RISK\ 0/nK} \qquad n = 10;\ k = 4,\ 8,\ \text{or}\ 12. \tag{24}$$

It was found that as NHS $\to \infty$ the σ_{EX} quickly converges into the above σ given by (21), (22), (23) respectively. Therefore, the graphic representation by printout taking the number of lines for NR is quite adequate.

In all of these cases, the FOM 1-1 and FOM 2-1 tend to zero for smaller σ as will be expected. Because of the central limit theorem, case (1) and (3) will approach to the case (2) in the region of high accuracy. In the cruder measurements where $\sigma \geq 1$, there may exist some deviation among them.

§3. Experimental results for two kinds of input data sets

As input data, we chose two examples;

(1) NOAF 7000

As is shown in Fig. 3, the first 4 lines, A, B, C, and D are the

same as the Shasi's Monte-Carlo results. As described earlier, eight more lines were arbitrarily added to know the possible effect of the number of element. We have three ways, parametrized by KR, to include as data;

KR = 1 4 lines, A ∿ D

KR = 2 8 lines, A ∿ H

KR = 3 12 lines, A ∿ L

(2) NOAF 4190

It consists of 12 identical horizontal lines given by

$f_{ij} = 0.500000$ for all i and j

An example of computer printout reproduced in Fig. 4.

We obtain from the three equation (21), (22), and (23)

$$\ell n\sigma_U = (n - NR)/2\cdot\ell n2 + (1/2)(\ell n\, f_{ij} + \ell n\,(1 - f_{ij})) \tag{25}$$

$$\ell n\sigma_G = (n - NR)\cdot\ell n2 = (m - MR)/2\cdot\ell n2 \tag{26}$$

$$\ell n\sigma_P = (n - NR)/2\cdot\ell n2 + \ell n\sqrt{f_{ij}} \tag{27}$$

As long as all the f_{ij} are of the same order of magnitude, we can substitute an average of $\ell n\sqrt{f_{ij}}$ for all i and j. Assuming $\bar{f}_{ij} = 0.5$, $\ell n\sqrt{f_{ij}} = -0.35$ in the unit of NR. Thus, by simply shifting somewhat to the right or to left the origin of abscissa, we can bring the $\ell n\sigma$ on the same scale and origin. As for the $\ell n\sigma_G$, we can also birng into the same scale by taking m and MR with

m = 2n and MR = 2NR, in the printouts like Fig. 4.

In all the experimental results, each point on the curve in Fig. 4 is the average of ten times repetition of random number generation, and in case of uniform, 10 × NHS times. Similar proceedure was repeated 6 times usually and are plotted on the same figure. The same results were also summarized in Figs. 5, 6, 7 & 8 in which all the FOM's were averaged and the abscissa is given in $\ell n\,(\sigma_{EX})$. We can notice from these results the following points;

(1) FOM 1-1 are larger than FOM 2-1 in all cases. Looking back at the equations (1) - (4)(17)(18), we can say that less room is left for the improvement by JSE proceedure by taking the regression lines of the raw experimental data.

(2) The uniform, normal and Poisson random number subroutines gave almost the same results in the region of

$$\sigma_{EX} \geqq 1$$

in case of NOAF 7000 at least for the input data.

(3) In the normal case, $\ell n(\overline{FOM\,i}-1)$ (i=1, 2) gave good linear relationship to $\ell n(NR)$, covering extremely wide range, that is, 1. to 0.0001 for FOM 1-1 and 0.3 to 0.0001 for FOM 2-1 corresponding to the range of standard deviation of 0.4 to 0.005, in case of KR = 1. (c.f. Fig.5).

(4) In the Poisson case, FOM-1 quickly decrease when the σ_{EX} become larger than the order of 1, showing somewhat flat maximum at around $\sigma_{EX} = 1.0$, at least for the case of KR = 1, 2. (c.f. Fig. 6.)

(5) In the region of $0.02 \leq$ FOM 1-1 $\lesssim 1.0$, the fluctuation of the resulting points is rather small whereas outside of this region and

also in all region for FOM 2-1, they show larger fluctuations. (c.f. Fig. 4).

(6) Even in the normal case, ℓn(FOM i-1) vs $\ell n\ \sigma_{EX}$ (i=1, 2) are not exactly linear. We can not neglect the tendency of bending down in the region of larger σ_{EX}. (c.f. Fig. 5).

(7) The remarkable depression of FOM (i - 1) (i=1, 2) in Poisson case for $\sigma_{EX} \geq 1$ can be understood by the fact that almost all of the A_{ij} will become zero.

(8) We have tried a modified Gaussian in which A_{ij} were put equal to zero if they come out to be negative, thus somewhat simulating the Poisson case. Fig. 5 shows that depression of FOM-1 occurs also, but not much as in the case of Poisson.

Roughly the same features are seen in the case of KR = 2 or 3, that is, the number of element is 8 or 12.

Similar experiments were done for the input data of NOAF 4190. Fig. 7, 8 are some typical results in this case. FOM 1-1 and FOM 2-1 are remarkably large in all three cases of uniform, normal and Poisson subroutines and look independent of NR or of standard deviations σ_{EX}, even though the fluctuation is also quite large. It looks, however, that they decrease somewhat in the region of larger standard deviation in case of Poisson as shown in Fig. 8. It is needed to repeat some more computer experiments to conclude more definitely.

Assuming horizontal straight lines for the FOM's vs NR, we have the values for the normal case as follows;

Table FOM's in the normal case

KR	FOM 1-1	FOM 2-1
1 (4 lines, A - D)	4.9	0.75
2 (8 lines, A - H)	19	5.4
3 (12 lines, A - L)	40	10.1

It looks that they are almost the same in the case of using Poisson.

§4. Monte-Carlo results compared with the computer simulation

In the following description we will refer mainly the results using normal random number. (case (2) in §2.)

To make the comparison of our simulated data with the Shasi's data more quantitatively, variance s^2 from the regression lines were computed for both case. s_j^2 is given as,

$$s_j^2 = \frac{\Sigma d_{y,x}^{\ 2}}{n-2} = \frac{1}{8}\{\Sigma(A_{ij} - \bar{y}_j)^2 - \frac{[\Sigma(x_i - \bar{x})(A_{ij} - \bar{y}_j)]^2}{\Sigma(x_i - \bar{x})^2} \qquad (28)$$

etc. (in the usual nomenclature) See (16).

The raw Shasi data gives for j=A, B, C, D

$$S_A^2 = 0.061, \quad S_B^2 = 0.098, \quad S_C^2 = 0.085, \quad S_D^2 = 0.065,$$

or in the unit given in Fig. 3,

$$S_A^2 = 0.00061, \quad S_B^2 = 0.00098, \quad S_C^2 = 0.00085, \quad S_D^2 = 0.00065,$$

and the experimental standard deviation defined by (24) to be

$$\sigma_{EX} = \sqrt{8/10}\sqrt{\sum_j S_j^2/4} = 0.025.$$

It corresponds in Fig. 5 to

FOM 1-1 = 0.0054

FOM 2-1 = 0.002

corresponding to $\sigma_{EX} = 0.025$. Thus the application of James-Stein Estimator for the Shasi's Monte-Carlo results will improve the data by the order of 0.5% for the FOM 1 and 0.2% for FOM 2 which are both very small.

It may be better to use Poisson subroutine to decide the FOM factor in the case like our Monte-Carlo results. Fig. 6, however, does not affect the results in such region, because of a certain technical limitations in our computer in Poisson case. However, due to the central limit theorem, the result will not differ from the case using normal subroutine.

§5. Discussion

Even though the present JSE procedure is not very powerful to the improvement of the current Shasi's data, it is highly possible that it becomes very powerful in some other cases. We can expect, for example, that it will be useful for a better estimation of the spectra

in case they are of very poor statistics because of very samll counting rate and the repetition of the measurements is not allowed.

To interpret the remarkable results of the linearity for log-log scale is left to the statistical theory. It is the task for forthcoming papers, where we will have to evaluate expectations, for example, of RISK 0 like

$$E(\text{RISK 0}) = \sum_{j=1}^{k} \sum_{i=1}^{n} E\,(A_{ij} - f_{ij})^2$$

$$= nk\sigma^2,$$

for $A_{ij} - f_{ij} \overset{\text{ind.}}{\sim} \mathcal{N}(0, \sigma^2)$. The computation of E(RISK 2) is less straightfoward but not difficult. However, to compute E(RISK 1), E(RISK 3) might be formidable tasks. Stochastic behavior of FOM 1, FOM 2 is thus almost intractable unless with proper, yet to find, approximations.

Acknowledements

One of the authors (M.K.) are grateful for the kind help of Mr. Kubota, Laboratory of Nuclear Science, Tohoku University and Dr. T. Kajitani, ANL, in programming. He is also much indebted to Prof. S. Sclove, University of Illinois, Chicago Circle, to his kind discussion. Authors thank Miss. Y. Nakayama, University fo Tsukuba (Inst. of Socio-Economic Planning), for her excellent typewriting of the manuscript.

Literatures

(1) Stein, C. Proceedings of the Third Berkeley Symposium on Mathematical Statistics and Probability, Vol,. Berkeley; University of California Press, 1955, 197 - 206.

(2) James, W. and Stein, C. ibid. 1961, 361 - 206.

(3) Efron, B. and Morris, C. Stein's Paradox in Statistics, Scientific American, May, 1977, 119 - 127.

(4) J. M. Capenter et al. IPNS project, Argonne National Laboratory Report 1975.

(5) IPNS-I, ANL78-88, p.126, Fig. 4.

Table 1

James-Stein Estimation of Monte-Carlo Result for the Data Shown in Fig. 2. (Hand calculated results)

$i = 1 \qquad x_i = \log E_i = 1.197$

A_1	$= 3.830 \times 10^{-4}$	C	$= 4.800$
$A_1^{(1)}$	$= 3.828$	$C^{(1)}$	$= 4.390$
A_2	$= 3.056$	B	$= 2.388$
$A_2^{(1)}$	$= 3.060$	$B^{(1)}$	$= 2.397$

Similar results are obtained for $i = 2, \ldots, 10$.

Figure Captions

Fig. 1. Schematic data of length measurements as a function of temperature for several metal pieces.

Fig. 2. Monte-Carlo results of IPNS target assembly. (Shasi's data for neutron spectra)

Fig. 3. Shasi's data with some arbitrarily added data set.

Fig. 4. An example of Computer print out (Case NOAF 7000, normal random number generator subroutine, FOM 1-1 vs NR)

Fig. 5. FOM 1-1, FOM 2-1 vs σ_{EX}(standard deviation) in log-log scale Case for normal and modified normal subroutine, NOAF 7000, KR = 1)

Fig. 6. FOM 1-1, FOM 2-1 vs σ_{EX}(Case for Poisson subroutine, NOAF 7000, KR = 1, 2, 3)

Fig. 7. FOM 1-1, FOM 2-1 vs σ_{EX}(Case for normal subroutine, NOAF 4190, KR = 1, 2, 3)

Fig. 8. FOM 1-1, FOM 2-1 vs σ_{EX}(Case for Poisson subroutine, NOAF 4190 KR = 1, 2, 3)

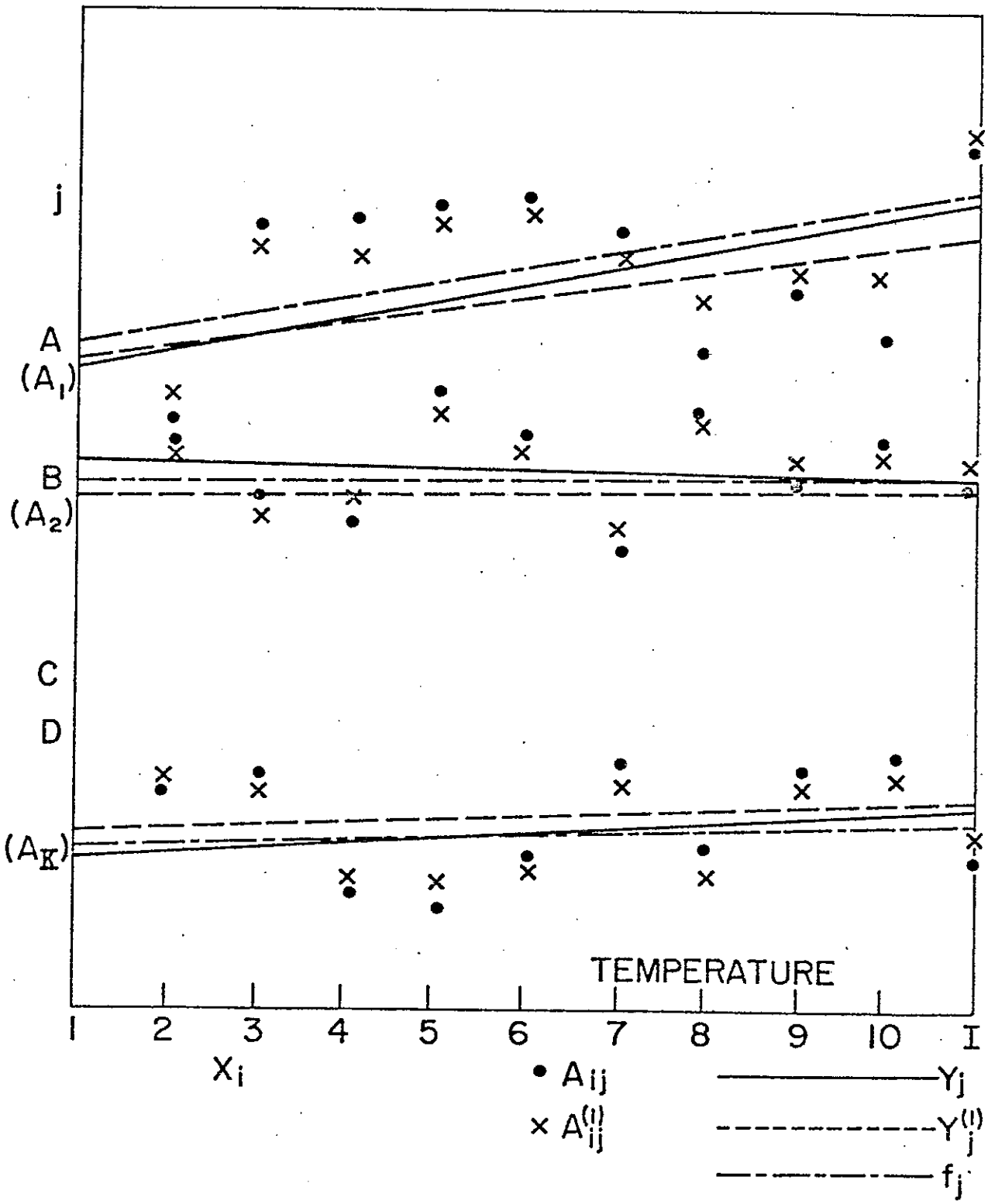
j
A
(A1)
B
(A2)
C
D
(AK)
TEMPERATURE
1
2
3
4
5
6
7
8
9
10
I
Xi
• Aij
× A(I)ij
Yj
Y(I)j
fj

Fig. 1

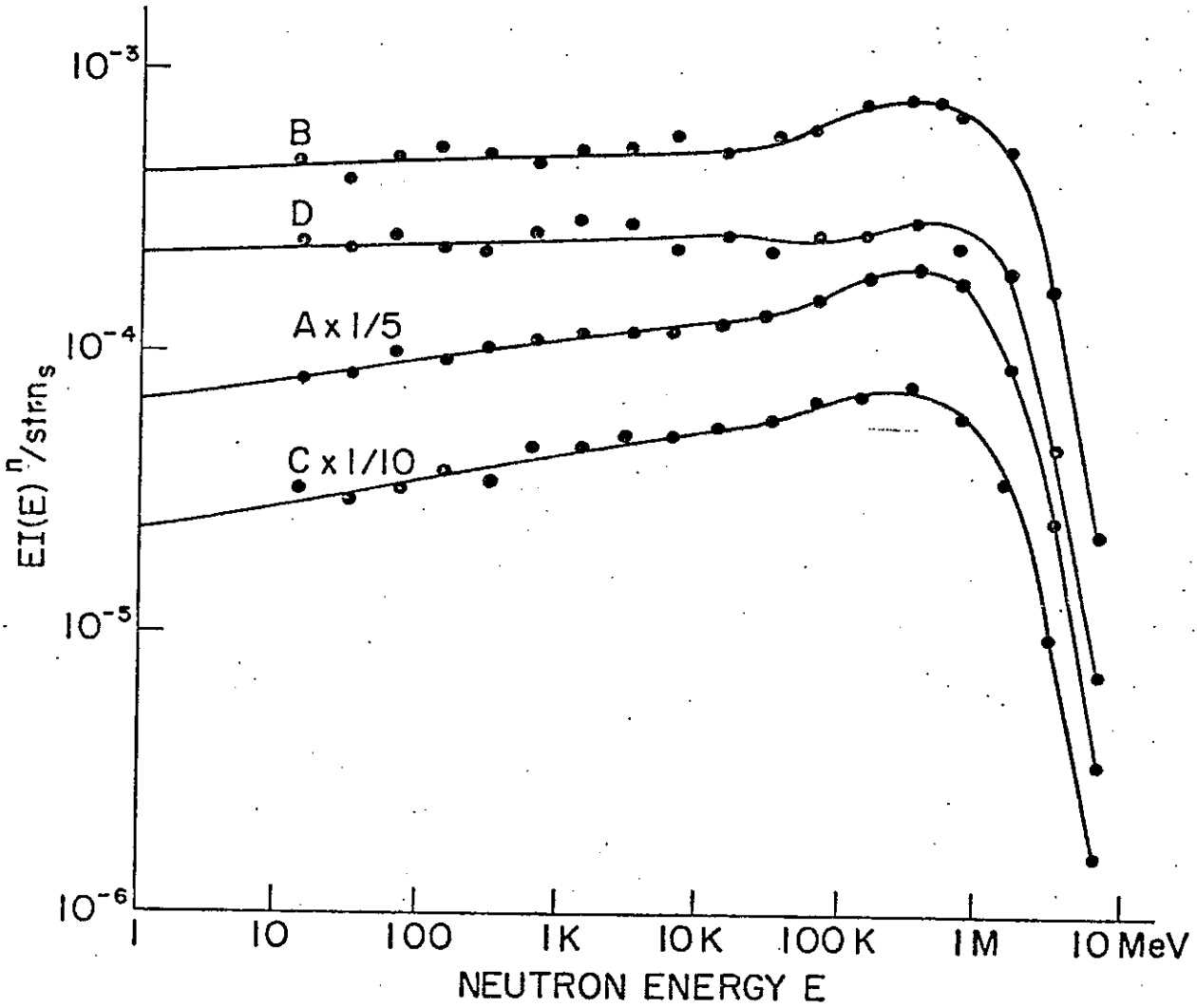
10^{-3}
10^{-4}
10^{-5}
10^{-6}
B
D
A x 1/5
C x 1/10
$EI(E)^{n}/str n_s$
1
10
100
1K
10K
100K
1M
10 MeV
NEUTRON ENERGY E

Fig. 2

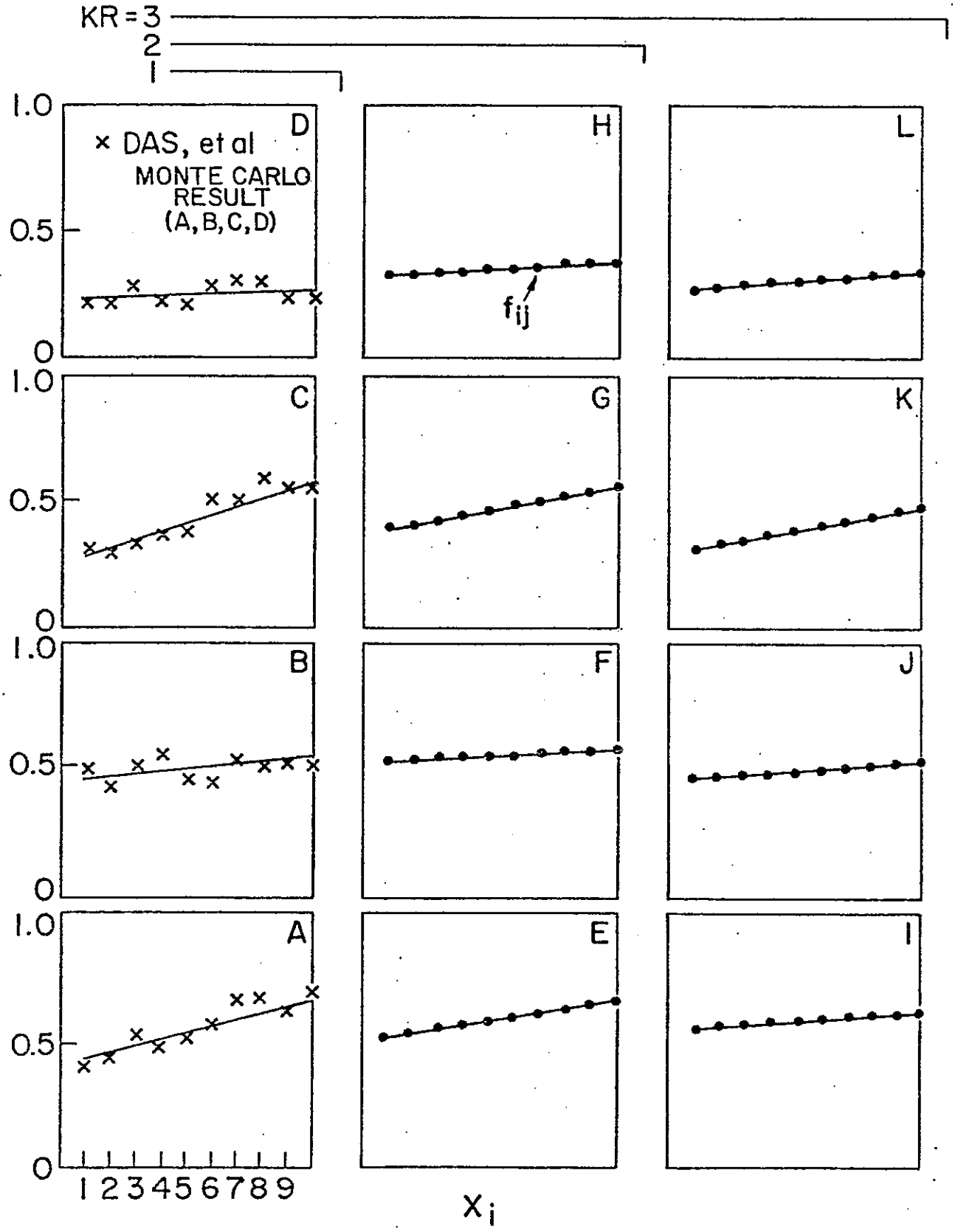
KR = 3
2
1
1.0
0.5
0
× DAS, et al
MONTE CARLO
RESULT
(A, B, C, D)
D
H
L
C
G
K
B
F
J
A
E
I
f_{ij}
1 2 3 4 5 6 7 8 9
X_i

Fig. 3

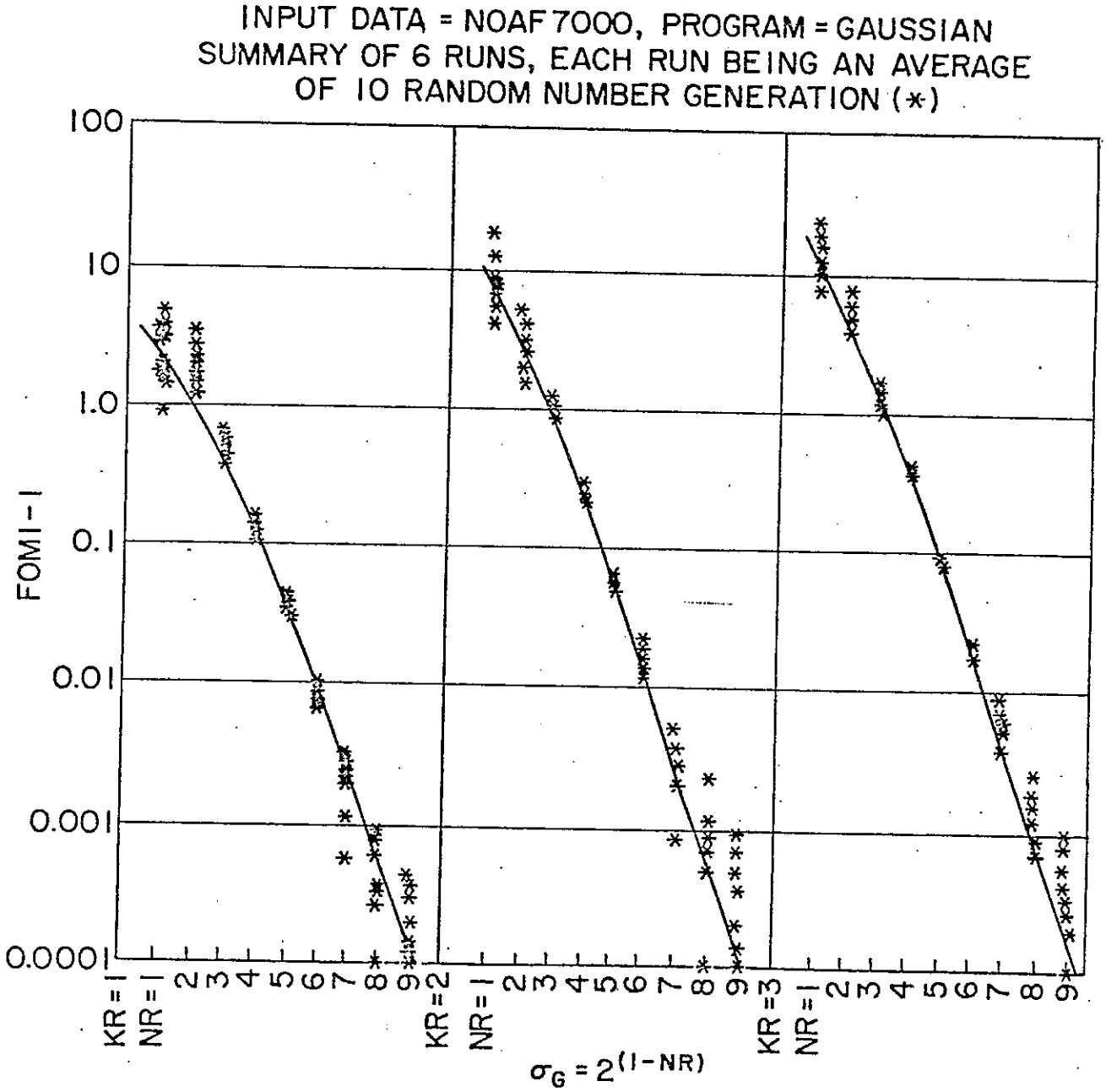
INPUT DATA = NOAF 7000, PROGRAM = GAUSSIAN
SUMMARY OF 6 RUNS, EACH RUN BEING AN AVERAGE
OF 10 RANDOM NUMBER GENERATION (*)
FOMI - I
100
10
1.0
0.1
0.01
0.001
0.0001
KR = 1
NR = 1 2 3 4 5 6 7 8 9
KR = 2
NR = 1 2 3 4 5 6 7 8 9
KR = 3
NR = 1 2 3 4 5 6 7 8 9
$\sigma_G = 2^{(1-NR)}$

Fig. 4

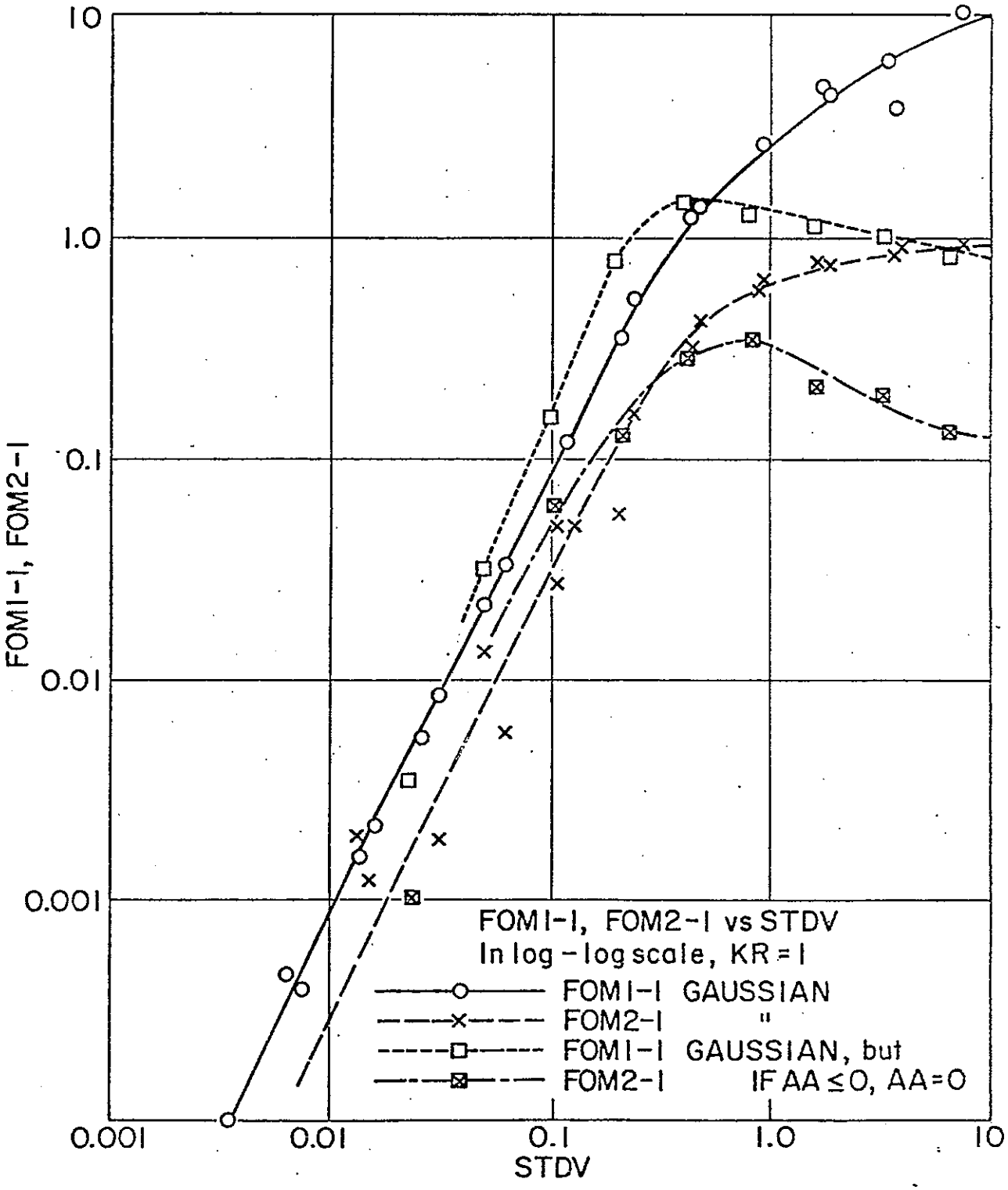
10
1.0
0.1
0.01
0.001
FOM1-1, FOM2-1
0.001
0.01
0.1
1.0
10
STDV
FOM1-1, FOM2-1 vs STDV
In log-log scale, KR=1
FOM1-1 GAUSSIAN
FOM2-1 "
FOM1-1 GAUSSIAN, but
FOM2-1 IF AA≤0, AA=0

Fig. 5

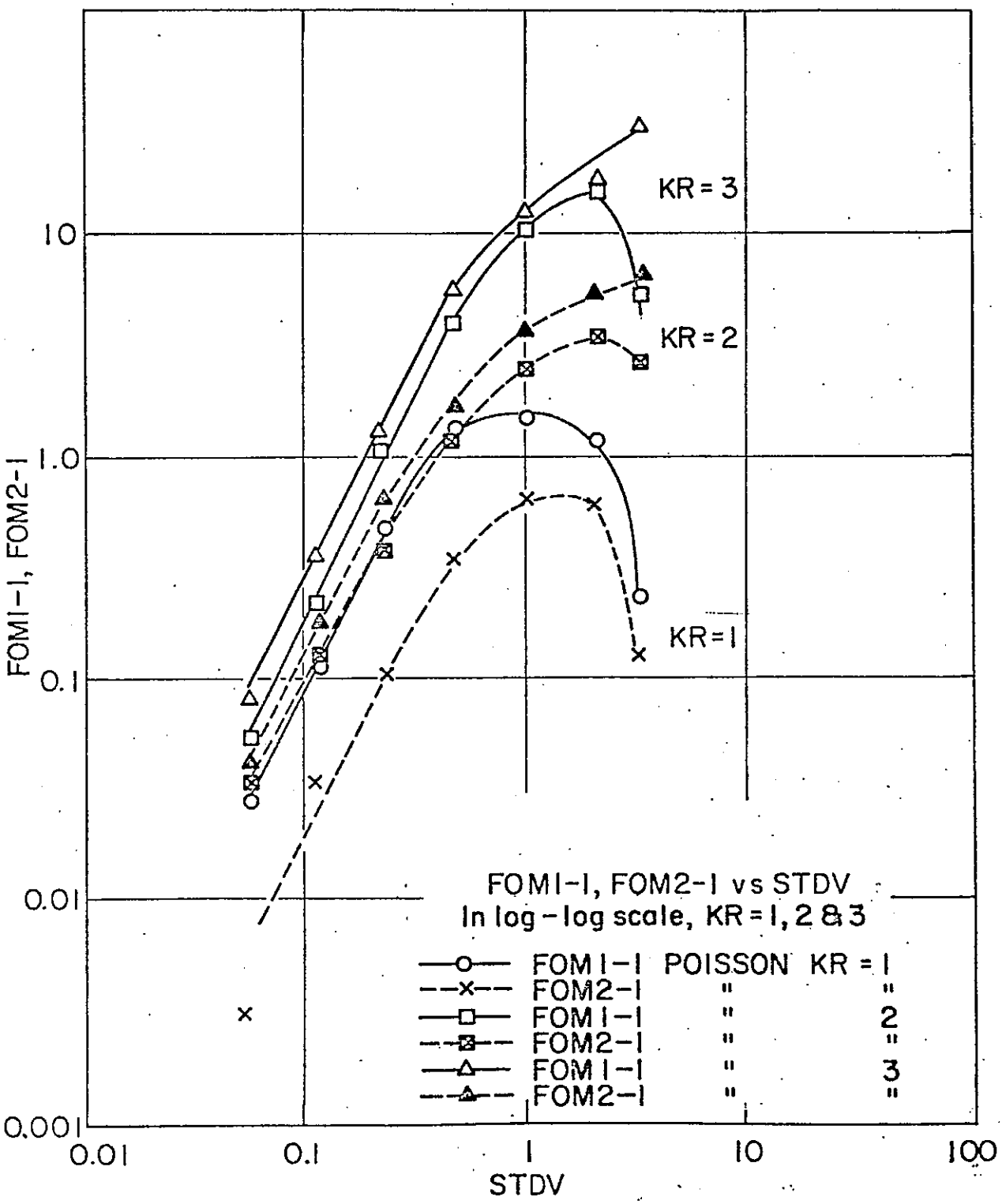
KR = 3
KR = 2
KR = 1
10
1.0
0.1
0.01
0.001
FOM1-1, FOM2-1
0.01
0.1
1
10
100
STDV
FOM1-1, FOM2-1 vs STDV
In log-log scale, KR = 1, 2 & 3
FOM1-1 POISSON KR = 1
FOM2-1 " "
FOM1-1 " 2
FOM2-1 " "
FOM1-1 " 3
FOM2-1 " "

Fig. 6

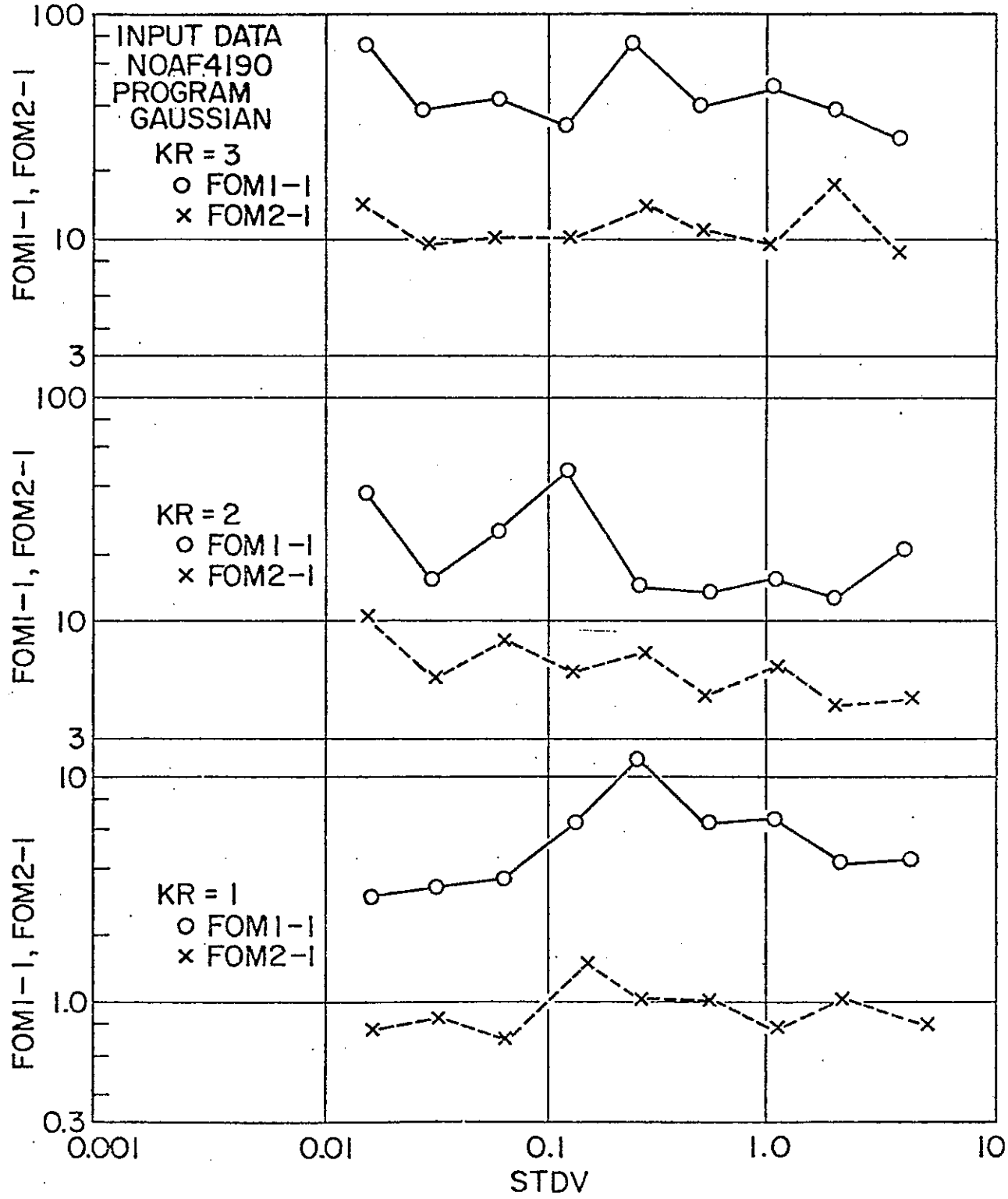
INPUT DATA
NOAF4190
PROGRAM
GAUSSIAN
KR = 3
o FOM1-1
× FOM2-1
KR = 2
o FOM1-1
× FOM2-1
KR = 1
o FOM1-1
× FOM2-1
FOM1-1, FOM2-1
100
10
3
1.0
0.3
0.001
0.01
0.1
1.0
10
STDV

Fig. 7

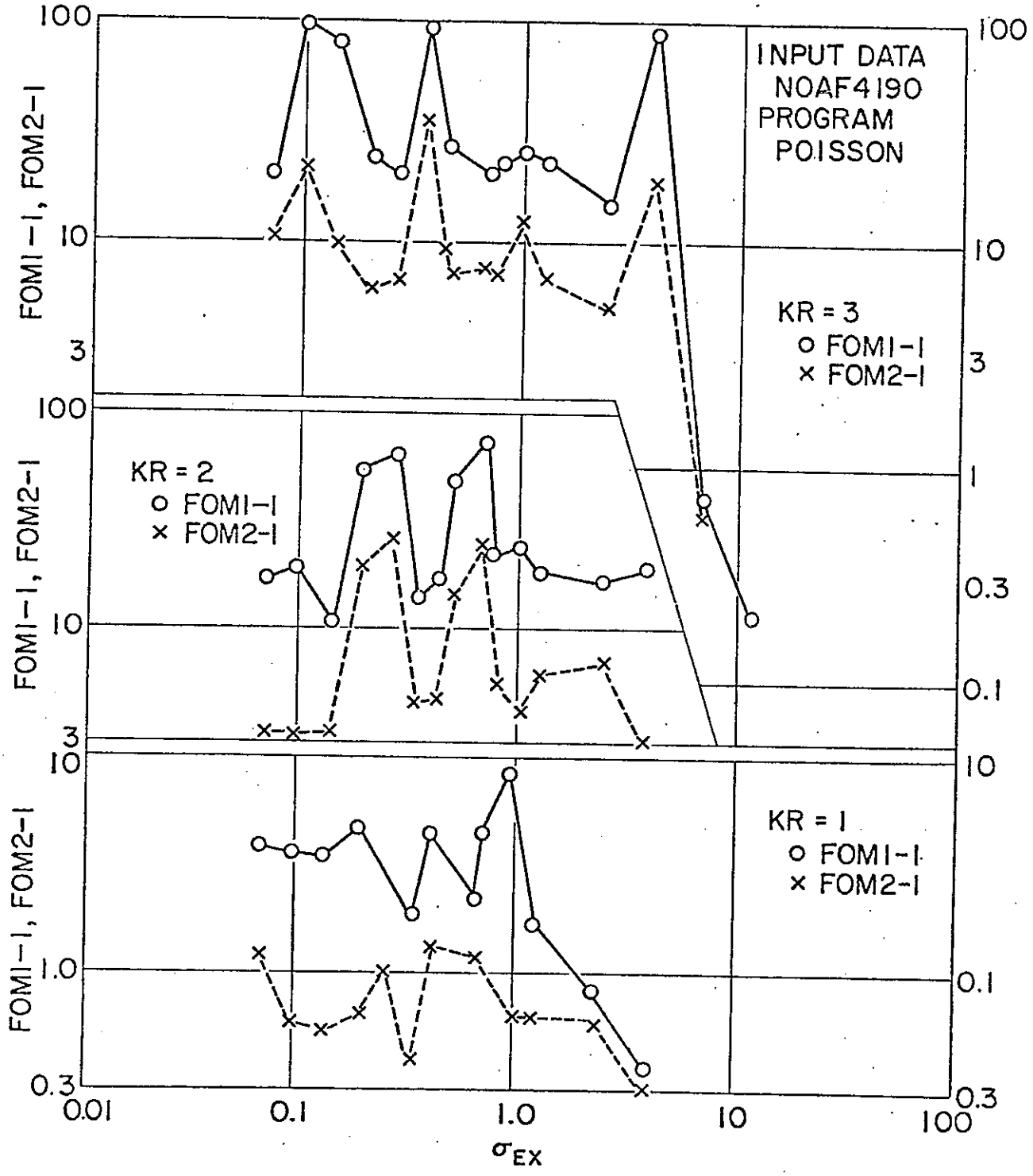
INPUT DATA
NOAF4190
PROGRAM
POISSON
KR = 3
o FOM1-1
× FOM2-1
KR = 2
o FOM1-1
× FOM2-1
KR = 1
o FOM1-1
× FOM2-1
FOM1-1, FOM2-1
100
10
3
1
0.3
0.1
1.0
0.01
0.1
1.0
10
100
σ_{EX}

Fig. 8